Advances in Materials
2015; 4(2-1): 9-13
Published online January 16, 2015 (http://www.sciencepublishinggroup.com/j/am)
doi: 10.11648/j.am.s.2015040201.12
ISSN: 2327-2503 (Print); ISSN: 2327-252X (Online)

Design of metal matrix composite with particle reinforcement

Seyed Ebrahim Vahdat*

Department of Engineering, Ayatollah Amoli Branch, Islamic Azad University, Amol, Iran

Email address:
e.vahdat@iauamol.ac.ir (S. E. Vahdat)

To cite this article:
Seyed Ebrahim Vahdat. Design of Metal Matrix Composite with Particle Reinforcement. *Advances in Materials*. Special Issue: Advanced Tool Steels. Vol. 4, No. 2-1, 2015, pp. 9-13. doi: 10.11648/j.am.s.2015040201.12

Abstract: Using the methods which are applied for estimating strength and toughness of composites reduces trial-and-error rate in their design. One of the mechanisms for strengthening and increasing toughness of composites is through debonding mechanism. Interface strength of reinforcement with matrix and effective surface of debonding greatly affect toughness and strength of these types of materials. In this study, a model was proposed to estimate the effect of interface and matrix strength of composites in increasing tensile toughness and strength. Then, interface strength and its effect in increasing tensile toughness and strength were calculated in a case study of composites containing particle reinforcement in matrix of steel.

Keywords: Interface, Tensile Toughness, Strength

1. Introduction

High-performance steels have high strength, hardness, abrasion resistance and toughness along with reasonable price. In general, hardness and strength are inversely related to toughness, which limits application of steels. In order to overcome this problem, engineers have started to produce composites with hard and abrasion resistant reinforcements. Factors such as adequate strength for the interface between reinforcement and matrix have challenged successful production of this type of material. Furthermore, uniformity of properties in these materials is a requirement for using very fine reinforcements that are almost finer than one micron and are highly dispersed, which leads to problems like agglomeration of reinforcement [1]. Similar to behavior of composites, scanning electron microscopy (SEM) image of debonding $M_{23}C_6$ particles from matrix of deep cryogenic treated 45WCrV7 [2] and AISI D2 [3] steels, and that of breaking down M_7C_3 particles have been observed [3]. Also, in force-displacement (F-ΔL) curve of deep cryogenic treated 1.2542 steel, the elastic part contains several slopes [4].

The focus of this study was the studying interface strength of reinforcement of $M_{23}C_6$ particles in matrix of AISI S1 steel so that this method could be generalized for fiber reinforcement. Moreover, in case debonding mechanism was active, how much would be effect of this mechanism in increasing strength and tensile toughness?

Using methods which are utilized for calculating strength and toughness of composites, trial-and-error rate was reduced in experimental production and designing these types of materials. Many models have been presented for estimating strength and toughness of composites with metal matrix and particle reinforcement. For instance, for the composite with aluminum matrix reinforced with 10 and 20% volume of alumina in similar conditions, fracture toughness has been reported to be in proportion to distance between the particles [5]. In other words, in a particular composite with similar interface in which volume fraction of particles is constant, the finer particles, the less distance between the particles would be; so, fracture toughness would be reduced. Nardone and Prewo estimated strength of composites with particle reinforcement by proposing an improved shear-lag model [6]. Shen et al. used finite element methods for composites with particle reinforcement to demonstrate that particle form had no significant impact on its tensile strength. They indicated that, in a composite with aluminum matrix (3.5% age hardened copper containing 20% volume of reinforcement) in similar conditions, strength decreased with cylindrical, spherical, defective cylindrical and two truncated cones, respectively [7]. In Hahn and Rosenfield's model, fracture toughness was directly related to size of particles, Young's modulus and yield strength of composite and inverse relationship with volume percent of particles [8]. In Garrett and Knott's model, fracture toughness was directly related to work hardening, Young's

modulus and yield strength of composite [8].

The above-mentioned models [5-8] are not based on microstructure; i.e. these models have ignored effect of particles population density and interface strength on load transfer. Therefore, interface strength between reinforcement particles and matrix and also effective surface of debonding particles were the research variables of the present work. By determining interface strength of reinforcement with matrix in certain operating conditions and controlling population density, size and content of reinforcement, desirable toughness and strength could be designed.

2. Experimental Methods

In this study, AISI S1 steel was utilized to calculate interface strength of reinforcement of $M_{23}C_6$ particles in matrix of steel. Accordingly, presenting a model for designing toughness and strength of AISI S1 steel in impact loading conditions is important in practical terms. Its chemical composition is listed in Table 1.

Table 1. *Chemical analysis of the AISI S1*

Element	(W%)	Element	(W%)	Element	(W%)	Element	(W%)	Element	(W%)	Element	(W%)
C	0.4800	Ni	0.1280	S	0.0250	W	1.5700	Mo	0.0281	Fe	Rest
Si	0.9950	V	0.0148	Cr	1.1200	Mn	0.3360	P	0.0567		

Table 2. *Content, average size and population density of M_7C_3 and $M_{23}C_6$ particles for AISI S1*

Code	M_7C_3 content	$M_{23}C_6$ content	M_7C_3 average size µm	$M_{23}C_6$ average size µm	population density of M_7C_3 mm^{-2}	population density of $M_{23}C_6$ mm^{-2}
241	0.42V%	2.18V%	0.5 (0.3to1)	0.22 (0.065to0.5)	62000	660000
242	0.47V%	2.42V%	0.55 (0.3to1)	0.23 (0.065to0.5)	65000	630000
243	0.37V%	3.73V%	0.7 (0.6to0.9)	0.28 (0.065to0.7)	60000	600000
361	0.57V%	4.69V%	0.65 (0.5to0.8)	0.30 (0.065to1)	64000	894000
362	0.60V%	6.92V%	0.7 (0.4to1.7)	0.35 (0.065to0.7)	63000	750000
363	0.34V%	8.91V%	0.7 (0.4to1.5)	0.40 (0.065to0.6)	62000	726000
481	0.35V%	10.04V%	0.7 (0.3to1.4)	0.24 (0.065to0.7)	65000	707000
482	0.25V%	12.66V%	0.7 (0.4to1.4)	0.5 (0.065to1)	62000	650000
483	0.24V%	12.87V%	0.7 (0.4to2)	0.52 (0.065to1)	65000	620000

To calculate interface strength, 9 sets of specimens, each of which included three specimens, were used for providing sufficient data for desirable conclusion and discussion. In order to determine microstructure characteristics, cylindrical specimens were 12 mm in diameter and 15 mm in length. TESCAN MIRA II device with EDS was used to obtain and analysis SEM images. In addition, OLYSIA m3 metallographic software which was calibrated for 2048 × 1536 pixels was utilized. For calculating each phase, at least 5 SEM images with magnification of 104 from one region were used. Mean of the data is reported in Table 2.

In accordance with BS EN 10002-1 standard [9], specimens of tensile test were prepared in dumbbell shape with diameter (d) of 5 mm, initial base length (L) of 25 mm and total length (L_t) of 15 cm; results are shown in Table 3.

Table 3. *Results of tensile test at room temperature for AISI S1*

Specimen code	$\sigma_{CO,UTS}$ MPa	ΔL_{CO} mm	U_T (MJ)= $2/3\times\sigma_{M,UTS}\times\Delta L_{CO}/50\times100$
241	2279±21	2.4±0.37	72.2
242	2265±31	1±0.5	30.2
243	2137±53	3±0.75	85.5
361	2268±65	3.5±0.75	*105.9*
362	2201±65	2.5±0.75	73.4
363	2245±65	2.5±0.75	74.8
481	2244±64	3.1±0.15	*92.8*
482	2206±65	3.8±0.75	*110.3*
483	2249±28	3.1±0.4	*93.0*

Tensile test was performed at a strain rate of 0.00166 s^{-1}. Machining of the specimens was implemented using a CNC milling device.

2.1. Theory

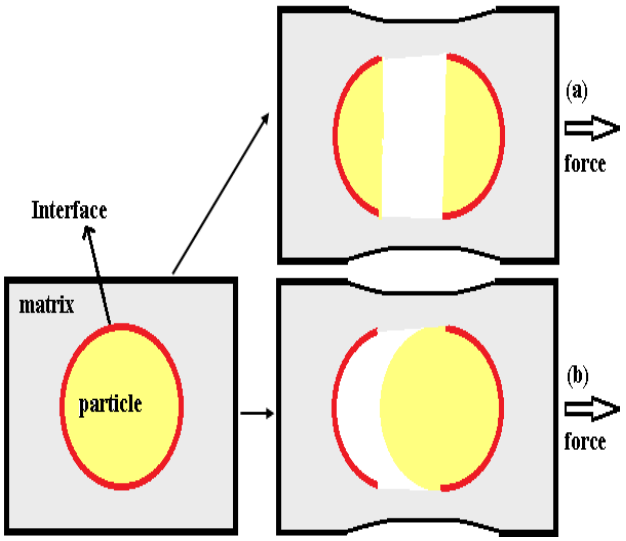

Figure 1. *Effective surface for strengthening (a) when particles are broken down (b) when particles are debonding*

To present a model for strength and tensile toughness of the composites with particle reinforcement in which debonding mechanism is dominant (Figure 1), if particles are broken down, the maximum effective surface will exceed the particle's diameter, which is equal to the circle area in spherical particles (Figure 1(a)). According to Figure 1(b), if

particles are debonding of the matrix (without being broken down), effective surface of the particle will be equal to its perimeter, and to surface of the sphere in spherical particles. In other words, when debonding mechanism is dominant, effective surface of particles increases for strengthening because circle area (πr^2) of each spherical particle is smaller than sphere surface ($4\pi r^2$).

2.2. Interface Strength is Less than that of Matrix and Particle

Interface has less strength; so, as long as particles are debonding from the matrix, the matrix along with debonding mechanism of particles plays a role in strengthening. Therefore, strength of composite is obtained using equations (1), (2) and (3). When the particles are debonding from the matrix, it will only resist until the composite is broken down.

$$A_{CO} = A_{P,ef} + A_{M,ef} \rightarrow A_{M,ef} = A_{CO} - PD \times \pi r^2 \quad (1)$$

$$\sigma_{CO,UTS} \times A_{CO} = (\sigma_{P,PO} \times A_{P,PO}) + (\sigma_{M,UTS} \times A_{M,ef}) \quad (2)$$

$$A_{P,PO} = PD \times 4\pi r^2 \quad (3)$$

By substituting equations (1) and (3) in equation (2), simplified equation (4) is obtained.

$$\sigma_{CO,UTS}=(\sigma_{P,PO} \times PD \times 4\pi r^2)+(\sigma_{M,UTS}\times(A_{CO}-PD\times\pi r^2)) \quad (4)$$

Toughness is the amount of work per volume unit of material before rupturing. Considering equation (5), it could be regarded as equivalent to the product of multiplying the force required for deformation by the length of pathway through which the particle is drawn in the matrix. If force is in Newton ($Force = \sigma \times A$) and the pathway is in meter, tensile toughness unit will be in Joule. Note that, length of the pathway through which the particle is drawn in the matrix ($2\pi r$) is in proportion to particle size. Considering Table 2 and 3, size of particles is very small (from 0.065 to 2 micron) and less than ΔL_{CO}.

$$U_T\equiv(\sigma_{P,PO}\times A_{P,PO}\times 2\pi r)+(\sigma_{M,UTS}\times A_{M,ef}\times \Delta L_{CO}) \quad (5)$$

By substituting equations (1) and (3) in equation (5), simplified equation (6) is obtained for calculating tensile toughness.

$$U_T\equiv(\sigma_{P,PO}\times PD\times 8\pi^2 r^3)+(\sigma_{M,UTS}\times(A_{CO}-PD\times\pi r^2)\times\Delta L_{CO}) \quad (6)$$

In equal conditions, tensile toughness of composites which are described above is higher than that of composites which are showed in Figure 1(a). This difference increases with increasing effective surface area of the debonding particles or surface area of interface ($A_{P,PO}$) and interface strength ($\sigma_{P,PO}$).

The first terms of equation (6) ($\sigma_{P,PO} \times PD \times 8\pi^2 r^3$) and equation (4) ($\sigma_{P,PO} \times PD \times 4\pi r^2$) are in fact effects of reinforcement debonding mechanism on increasing tensile toughness and strength, respectively.

3. Results and Discussion

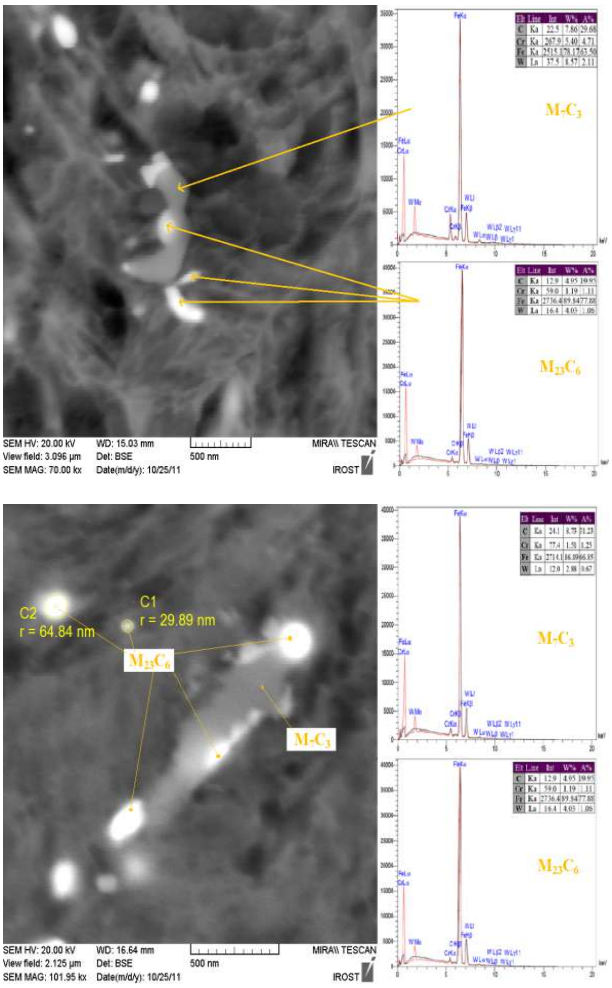

Figure 2. *Composition, morphology and size of carbides*

Figure 2 shows SEM images of the composition, morphology and size of carbides.

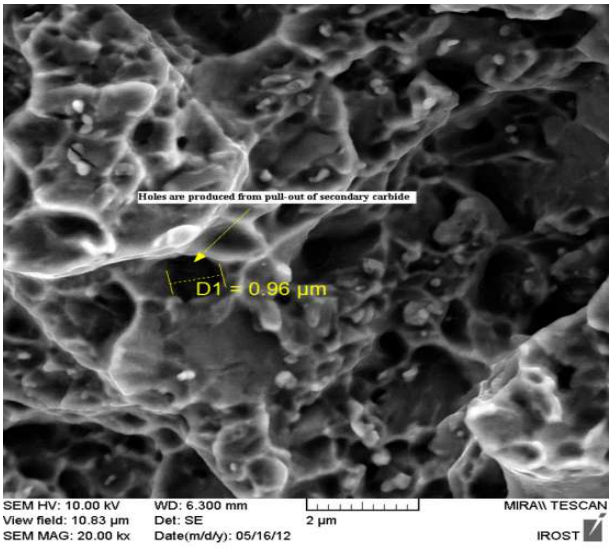

Figure 3. *SEM image of the necking area of specimen 482, ×20000, after ultrasonic cleaning*

Figure 3 shows SEM image of the necking area of specimen 482 using secondary electron gun. It shows pull-out of carbide of 0.96 μm in diameter that produced micro-void during tensile test because of carbide pull-out.

M_7C_3 particles were broke down but $M_{23}C_6$ particles were debonding; so, effects of M_7C_3 particles on calculating tensile toughness and strength based on debonding mechanism were neglected. Additionally, volume fraction of $M_{23}C_6$ particles was much higher than that of M_7C_3 particles (Table 2). On the other hand, condition of Figure 1(a) never happened. In condition of Figure 1(b), four factors contributed to increased tensile toughness and strength of the studied composite, which included matrix strength, interface strength, matrix surface and interface surface.

The amount of debonding surface with a role in strengthening was calculated for $M_{23}C_6$ particles using equation (3) per square meter of composite surface ($A_{CO}=1m^2$), as listed in Table 4.

Effective surface of the matrix was obtained by subtracting composite surface ($1m^2$) from total surface of particles, equation (1), as given in Table 4. Accordingly, values of two factors were determined. According to the data in Tables 2 and 3, solving equation (4) and (6) in a system of two equations with two unknowns led to determining two other factors of matrix strength ($\sigma_{M,UTS}$) and interface strength ($\sigma_{P,PO}$) based on equations (7) and (8), the values of which are listed in Table 4.

$$\sigma_{P,PO}=(\sigma_{CO,UTS}-\sigma_{M,UTS}\times(1-PD\times\pi r^2))/(PD\times 4\pi r^2) \quad (7)$$

$$\sigma_{M,UTS}=((U_T/14.7)-2\pi r\times\sigma_{CO,UTS})/((\Delta L_{CO}-2\pi r)\times(1-PD\times\pi r^2)) \quad (8)$$

Effect of debonding mechanism of $M_{23}C_6$ particles in matrix of AISI S1 steel on increasing tensile toughness, i.e. the first term of equation (6), was calculated (recorded in Table 4), which was negligible since particle reinforcements had small effective surface for tensile toughness ($PD\times 4\pi r^2\times 2\pi r$) whereas fiber reinforcements had much larger effective surface for tensile toughness ($PD\times 2\pi rL/2\times L/2$). For example, in equal conditions, if fiber length was at least 300 times of fiber radius ($L=300\times r$), then effective surface for tensile toughness would be 1800 ($\approx 300^2/16\pi$). However, effect of debonding mechanism of $M_{23}C_6$ particles in matrix of AISI S1 steel on increasing strength, i.e. the first term of equation (4) (in accordance to Table 4), would be 9.3%, which was considerable.

As represented in Figure 4, in all the specimens except 241, strength of interface was less than that of the matrix. This issue provided the field for debonding particles; i.e. it was in agreement with the initial assumption that was governing condition of Figure 1(b). On the other hand, interface strength was being reduced because, size of $M_{23}C_6$ particles became larger (according to Table 3); larger particles decreased coherency of interface, which reduced strength of the interface.

Table 4. *Deboning surface, matrix surface, strength of matrix, strength of interface and effect of debonding mechanism in increasing strength and tensile toughness*

Code	$A_{P,PO}$ mm^2	$A_{M,ef}$ mm^2	Matrix strength	Interface strength	Effect of reinforcement debonding mechanism in increasing tensile toughness, the first term of equation (6) ($\sigma_{P,PO}\times PD\times 8\pi^2r^3$)	Effect of reinforcement debonding mechanism in increasing strength, the first term of equation (4) ($\sigma_{P,PO}\times PD\times 4\pi r^2$)
241	100304	974924	2099	2317	----------	----------
242	104647	973838	*2109*	*2012*	2238J (0.007%)	211MPa (9.3%)
243	147706	963074	*2012*	*1344*	2570J (0.003%)	199MPa (9.3%)
361	252644	936839	*2195*	*834*	2922J (0.003%)	211MPa (9.3%)
362	288488	927878	*2151*	*709*	3309J (0.005%)	205MPa (9.3%)
363	364742	908814	*2240*	*572*	3857J (0.005%)	209MPa (9.3%)
481	429788	892553	*2280*	*485*	4241J (0.005%)	209MPa (9.3%)
482	510250	872438	*2293*	*402*	4738J (0.004%)	205MPa (9.3%)
483	526415	868396	*2349*	*397*	5024J (0.005%)	209MPa (9.3%)

According to Table 4, effect of debonding mechanism on increasing strength was the same (9.3%) for all the specimens since (as demonstrated in Table 3) all of them had almost equal strength.

According to Figure 4, interface strength (from 2012 to 397 MPa) was smaller than matrix strength (from 2012 to 2349 MPa) in all the specimens, except specimen 241. Therefore, conditions were appropriate for activating debonding mechanism. Moreover, according to Table 2, in the studied steel, debonding mechanism of the reinforcement particles had a negligible effect (0.003 to 0.007%) on increasing tensile toughness; this effect was considerable in the case of tensile strength (9.3%).

According to Table 2, the amount of secondary carbide constantly increased. Thus, the matrix metal around the carbide had poor carbon and alloying elements. Accordingly, the matrix which was poor in carbon and alloying elements could have an effective role in increasing tensile toughness.

For strength, the above finding was confirmed in Figure 4, strength of metal matrix is almost constant. Therefore, strengthening of debonding mechanism had the significant effect on strength of composite.

This method can be generalized to the composite with fiber reinforcement. In such a state, equations (7) and (8) can be changed as equations (9) and (10).

$$\sigma_{fiber,PO}=(\sigma_{CO,UTS}-\sigma_{M,UTS}\times(1-PD\times\pi r^2))/(PD\times\pi DL/2) \quad (9)$$

$$\sigma_{M,UTS}=((U_T/K)-L/2\times\sigma_{CO,UTS})/((\Delta L_{CO}-L/2)\times(1-PD\times\pi r^2)) \quad (10)$$

Whereas D is fiber diameter, L is fiber length and K is equality coefficient of equation (6).

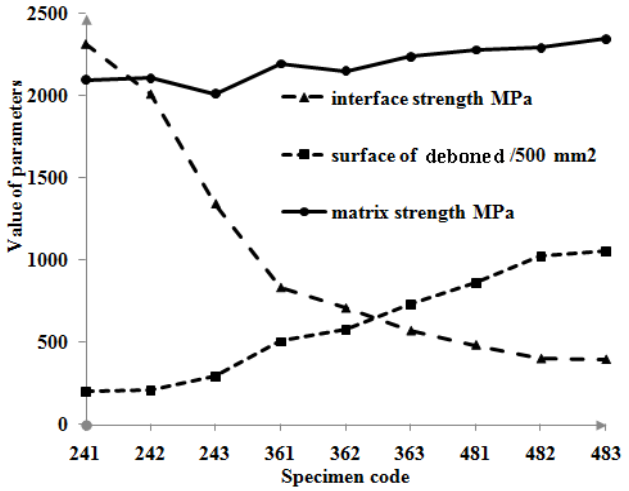

Figure 4. *Comparing debonding surface, matrix strength and interface strength for 9 different specimens*

4. Conclusions

In this study, a method was proposed for designing tensile toughness and strength of composites based on reinforcement debonding mechanism. In this method, simultaneous increase of tensile strength and tensile toughness occurred when interface strength was less than matrix strength and reinforcement strength. This method was utilized for 9 specimen sets of AISI S1 steel with particle reinforcement. Considering mean diameter of spherical particles, it could be concluded that:

1. Debonding mechanism had a negligible effect on increasing tensile toughness of composite with particle reinforcement.

2. Debonding mechanism had a considerable effect on increasing tensile strength of composite with particle reinforcement.

Nomenclature

A_{CO} = Surface of composite = $1m^2$
$A_{M,ef}$ = Effective surface of matrix
$A_{P,PO}$ = Effective surface of debonding
$A_{P,ef}$ = Effective surface of particle
$\sigma_{M,UTS}$ = Ultimate tensile strength of matrix
$\sigma_{CO,UTS}$ = Ultimate tensile strength of composite
$\sigma_{P,UTS}$ = Ultimate tensile strength of particle
$\sigma_{P,PO}$ = Interface strength
e_f = Fracture strain
ΔL_{CO} = Elongation of composite
L= Length of fiber
R= Particle radius

References

[1] S. Cory A., Ed., *Discontinuous reinforcement for metal-matrix composites*, (ASM International, Ohio, 2000), vol. 21, pp. 131.

[2] S. E. Vahdat, S. Nategh and S. Mirdamadi, "Microstructure and tensile properties of 45WCrV7 tool steel after deep cryogenic treatment," *Materials Science and Engineering: A* Vol. 585, pp. 444-454, 2013.

[3] D. Das and K. K. Ray, "Structure–property correlation of sub-zero treated AISI D2 steel," *Materials Science and Engineering: A* Vol. 541, pp. 45-60, 2012.

[4] F. Farhani, K. S. Niaki, S. E. Vahdat and A. Firozi, "Study of effects of deep cryotreatment on mechanical properties of 1.2542 tool steel," *Materials & Design* Vol. 42, pp. 279-288, 2012.

[5] N. Chawla and J. E. Allison, Eds., *Fatigue of Particle Reinforced Materials*, (Elsevier, Oxford, 2001), pp. 2967-2971.

[6] V. C. Nardone and K. M. Prewo, "On the strength of discontinuous silicon carbide reinforced aluminum composites," *Scripta Metallurgica* Vol. 20, pp. 43-48, 1986.

[7] Y. L. Shen, E. Fishencord and N. Chawla, "Correlating macrohardness and tensile behavior in discontinuously reinforced metal matrix composites," *Scripta Materialia* Vol. 42, pp. 427-432, 2000.

[8] S. Bhaskar, Majumdar, S., Ed., *Engineering mechanics and analysis of Metal Matrix Composite*, (ASM International, Ohio, 2000), vol. 21, pp. 975.

[9] B.S., 10002–1, Metallic materials tensile testing, Part 1: method of test at ambient temperature, 2001